Weak localization of holes in high-mobility heterostructures

F. V. Porubaev and L. E. Golub[*]

Ioffe Physical-Technical Institute of the Russian Academy of Sciences, 194021 St. Petersburg, Russia
(Received 25 June 2012; revised manuscript received 22 November 2012; published 9 January 2013)

Theory of weak localization is developed for two-dimensional holes in semiconductor heterostructures. Ballistic regime of weak localization where the backscattering occurs from few impurities is studied with account for anisotropic momentum scattering of holes. The transition from weak localization to antilocalization is demonstrated for long dephasing times. For stronger dephasing the conductivity correction is negative at all hole densities due to nonmonotonous dependence of the spin relaxation time on the hole wavevector. The anomalous temperature dependent correction to the conductivity is calculated. We show that the temperature dependence of the conductivity is nonmonotonous at moderate hole densities.

PACS number(s): 73.20.Fz, 73.21.Fg, 75.70.Tj, 72.25.Rb

I. INTRODUCTION

Weak localization (WL) is an enhancement of backscattering caused by interference of waves propagating by the same path in the opposite directions. WL of electrons results in corrections to conductivity anomalously dependent on temperature and magnetic field. Weak localization is studied in a variety of disordered metals and semiconductors including recently discovered graphene and topological insulators. In these systems, the carrier momentum is coupled strongly with spin or pseudospin which results in nonparabolic energy spectrum. This leads to suppression of the backscattering called weak antilocalization (WAL). WAL is observed in graphene (for review see Ref. [1]) and in topological insulators[2–5] (the corresponding theory is developed in Refs. [6] and [7]).

Heterostructures with hole type of conductivity also belong to the class of systems with nonparabolic energy spectrum and coupled spin and orbital degrees of freedom. Since the two-dimensional valence band states are formed as a result of competition of size quantization and strong spin-orbit interaction present in the bulk semiconductor, the spectrum nonparabolicity depends on the two-dimensional hole density p and the quantum well width a. At small density and in narrow structures the holes behave as ordinary electrons, while at $pa^2 \geqslant 1$ the nonparabolicity effects are important and spin is strongly coupled with the momentum. This leads to transition from WL at low density to WAL at higher densities in 2D hole systems caused by increase of spin-orbit strength.[8]

Experimental studies showed the WL-WAL transition with increase of 2D hole density in both temperature and magnetic-field dependences of the conductivity.[9–12] The WL theory for hole systems[13–15] was developed for the so-called "diffusion" regime where the backscattering occurs after many collisions with impurities. The diffusion theory describes well the magnetoconductivity in low-mobility hole structures,[16] but it is inapplicable to high-mobility systems studied nowadays because it describes magnetoconductivity in very low fields.

The temperature dependence of the conductivity is also different in high-mobility systems. WL is present due to these closed paths where the interference is not broken by dephasing processes. This means that the phase breaking time τ_ϕ should be much longer than the momentum scattering time τ. However, the diffusion theory of WL assumes a stronger condition $\ln(\tau_\phi/\tau) \gg 1$ which is not realized in high-mobility structures with long scattering times. The backscattering in these systems occurs after carrier propagation along "ballistic" paths with few impurities which are ignored by the diffusion theory.[17,18] The aim of this work is to develop the WL theory of two-dimensional holes valid in both the diffusion and ballistic regimes and calculate the temperature dependence of the conductivity correction.

II. HOLE WAVEFUNCTIONS AND RELAXATION TIMES

The hole states in quantum-well structures grown from A_3B_5 materials are described by the Luttinger Hamiltonian where the wavevector component k_z is treated as an operator $-i\partial/\partial z$ (here z is the growth direction).[19] We apply the isotropic approximation and assume the quantum well to be rectangular and infinitely deep. We have found the hole energy dispersion in the subbands of size quantization in this model by a standard way.[19] The dependence of the hole energy in the ground subband on the two-dimensional wavevector $E(k)$ is nonparabolic at $ka \geqslant 2$, see inset to Fig. 1. Hereafter we use in numerical calculations the Luttinger parameters corresponding to GaAs: $\gamma_1 = 6.8$ and $\gamma_2 = \gamma_3 = 2.6$.

The size-quantized hole levels in a symmetrical quantum well are double degenerate at each value of $\boldsymbol{k}$. We choose these two states as symmetric (s) and asymmetric (a) relative to a mirror reflection in the symmetry plane of the quantum well.[20] The corresponding wave functions are $\Psi_{\alpha k} = F_{\alpha k}(z) \exp(i\boldsymbol{k} \cdot \boldsymbol{\rho})$, where $\boldsymbol{\rho}$ is the in-plane coordinate, $\alpha = s,a$, and $F_{\alpha k}(z)$ are linear superpositions of the four Bloch functions u_m of the total angular momentum 3/2 and projections on the growth axis $m = \pm 3/2, \pm 1/2$: $u_{\pm 3/2} = \mp(X \pm iY)s_\pm/\sqrt{2}$, $u_{\pm 1/2} = [\mp(X \pm iY)s_\mp/\sqrt{2} + \sqrt{2}Zs_\pm]/\sqrt{3}$. Here X,Y,Z are the Bloch functions of the top of the valence band, and $s_\pm$ are spin functions with projections $\pm 1/2$ on the z axis. In the basis $[u_{3/2}, u_{1/2}, u_{-1/2}, u_{-3/2}]$, $F_{\alpha k}$ have the following form:[13,20]

$$F_{sk}(z) = [-v_0 C(z), iv_1 S(z)e^{i\varphi_k}, -v_2 C(z)e^{2i\varphi_k}, iv_3 S(z)e^{3i\varphi_k}],$$
(1)

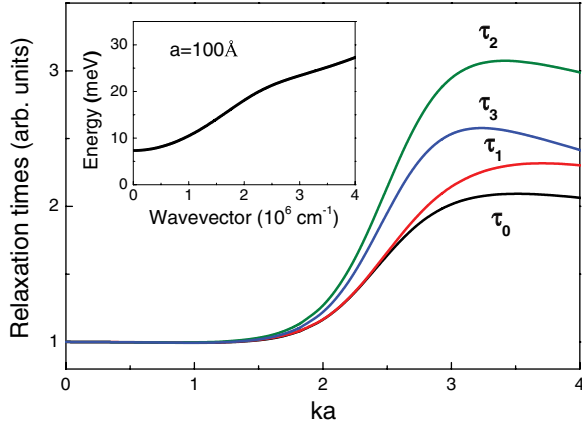$$F_{ak}(z) = [iv_3 S(z)e^{-3i\varphi_k}, v_2 C(z)e^{-2i\varphi_k}, iv_1 S(z)e^{-i\varphi_k}, v_0 C(z)],$$
(2)

FIG. 1. (Color online) Elastic relaxation times of holes. Inset: energy dispersion of the ground hole subband in a 100 Å wide quantum well.

where φ_k is the polar angle of the wavevector $\boldsymbol{k}$. The dependence on k of the real coefficients $v_{0...3}$ as well as symmetric (C) and antisymmetric (S) functions of the coordinate z is determined by the energy dispersion $E(k)$.

In Ref. 21 the phase-coherent transport through two-dimensional hole systems has been considered. The Luttinger Hamiltonian has been averaged over the ground state at $k = 0$ which resulted in its splitting into two blocks. This approach takes into account only the mixing between the $\pm 3/2$ and $\mp 1/2$ states whose angular momentum z projections differ by $\Delta m = \pm 2$, but ignores the mixing between the $\pm 3/2$ and $\pm 1/2$ states with $\Delta m = \pm 1$ which is of the same order. As a result, Ref. 21 takes into account only one part of k^2 terms in the WL conductivity correction. In the present work we use the whole 4×4 Hamiltonian and work with the four-component functions Eqs. (1) and (2), as it has been done for the diffusive regime in Refs. 13–15.

We consider elastic scattering of two-dimensional holes by the short-range potential $V(\boldsymbol{r}) = V_0 \sum_i \delta(\boldsymbol{r} - \boldsymbol{r}_i)$, where $\boldsymbol{r}_i = (\boldsymbol{\rho}_i, z_i)$ are coordinates of the impurities. The spin-orbit coupling leads to anisotropy of scattering even by such isotropic impurities. Indeed, the hole wave functions Eqs. (1) and (2) depend on a direction of the wavevector $\boldsymbol{k}$. As a result, the matrix elements of scattering from the state $|\alpha \boldsymbol{k}\rangle$ to the state $|\beta \boldsymbol{k}'\rangle$ by the potential $V(\boldsymbol{r})$

$$V_{\beta \alpha}(\varphi_{k'}, \varphi_k) = V_0 \sum_i F_{\beta k'}^\dagger(z_i) F_{\alpha k}(z_i) e^{i(\boldsymbol{k} - \boldsymbol{k}') \cdot \boldsymbol{\rho}_i}$$

depend on the angular coordinates of the initial and final wavevectors φ_k and $\varphi_{k'}$. Therefore the elastic scattering probability contains the first, second, and third Fourier harmonics of the scattering angle $\theta = \varphi_{k'} - \varphi_k$ in addition to the isotropic term. Hence the scattering times describing decay of the nth Fourier harmonics of the hole distribution function

$$\frac{1}{\tau_n} = \frac{2\pi}{\hbar} g \int_0^{2\pi} \frac{d\theta}{2\pi} \langle |V_{ss}(\theta)|^2 + |V_{as}(\theta)|^2 \rangle (1 - \cos n\theta)$$

are different for $n = 1, 2, 3$. All higher harmonics decay with the time τ_0 given by

$$\frac{1}{\tau_0} = \frac{2\pi}{\hbar} g \int_0^{2\pi} \frac{d\theta}{2\pi} \langle |V_{ss}(\theta)|^2 + |V_{as}(\theta)|^2 \rangle.$$

Here angular brackets denote averaging over the impurity positions, and $g = k/(2\pi\hbar v_k)$ is the density of states where $v_k = \hbar^{-1} dE/dk$ is the velocity of holes with the wavevector k. The dependences $\tau_n(k)$ for $n = 0, 1, 2, 3$ are plotted in Fig. 1 for homogeneous impurity distribution over the z coordinate (averaging is restricted to integration over z_i). The longest time is τ_2 describing a decay of the anisotropic part of the distribution function $\propto \cos 2\varphi_k$, $\sin 2\varphi_k$ which can be created, e.g., by optical excitation of semiconductor systems. Figure 1 demonstrates that $\tau_2 > \tau_1$, i.e., this part lives longer than the first harmonic $\propto \cos \varphi_k$, $\sin \varphi_k$ which can be created by application of an external static electric field. Figure 1 demonstrates that the p-type heterostructures differ qualitatively from topological insulators and graphene where scattering is also anisotropic, but the ratios $\tau_1/\tau_0 = 2$, $\tau_n/\tau_0 = 1$ (for $n > 1$) are fixed, and all relaxation times are independent of k. In contrast, the spin-orbit coupling is absent for holes at $k \to 0$, where the spectrum is parabolic and scattering is isotropic, while at $ka \gtrsim 2$ both conditions are violated. This implies the spin-orbit coupling strength in the hole systems is controlled by the density p which sets the Fermi wavevector $k_F = \sqrt{2\pi p}$.

III. WL CONDUCTIVITY CORRECTION

The anisotropy of scattering complicates the calculation of the WL conductivity correction. It is determined by the Cooperon $C_{\gamma\delta}^{\alpha\beta}(\varphi_k, \varphi_{k'}, \boldsymbol{q})$ which depends on the four indexes enumerating the hole states ($\alpha, \beta, \gamma, \delta = s, a$), on the directions of the momenta at the Fermi circle $\varphi_k, \varphi_{k'}$, and on the two-dimensional vector $\boldsymbol{q}$, $q \ll k_F$. The Cooperon satisfies the equation[13,22]

$$C_{\gamma\delta}^{\alpha\beta}(\varphi_k, \varphi_{k'}, \boldsymbol{q}) = W_{\gamma\delta}^{\alpha\beta}(\varphi_k, \varphi_{k'}) + \int_0^{2\pi} \frac{d\varphi_1}{2\pi} P(\varphi_1, \boldsymbol{q})$$
$$\times W_{\gamma\nu}^{\alpha\mu}(\varphi_k, \varphi_1) C_{\nu\delta}^{\mu\beta}(\varphi_1, \varphi_{k'}, \boldsymbol{q}), \quad (3)$$

where

$$P(\varphi_1, \boldsymbol{q}) = \frac{2\pi g_F \tau_0 / \hbar}{1 - i q v_F \tau_0 \cos(\varphi_1 - \varphi_q) + \tau_0 / \tau_\phi},$$

g_F and v_F are the density of states and the velocity at $k = k_F$, and the correlators are defined as

$$W_{\gamma\delta}^{\alpha\beta}(\varphi_k, \varphi_{k'}) = \langle V_{\alpha\beta}(\varphi_k + \pi, \varphi_{k'} + \pi) V_{\gamma\delta}(\varphi_k, \varphi_{k'}) \rangle. \quad (4)$$

For scattering in a symmetrical quantum well the correlators have the properties following from Eqs. (1) and (2):

$$\begin{aligned} W_{ss}^{ss} &= \left(W_{aa}^{aa}\right)^*, & W_{aa}^{ss} &= W_{ss}^{aa}, \\ W_{sa}^{sa} &= \left(W_{as}^{as}\right)^*, & W_{as}^{sa} &= W_{sa}^{as}, \end{aligned} \quad (5)$$

and all other correlators are equal to zero. Note that the relaxation times are determined by $\langle |V_{ss}|^2 + |V_{as}|^2 \rangle = W_{ss}^{ss} - W_{as}^{sa}$. The correlators contain Fourier harmonics $\exp(\pm i m\varphi_k \pm i n\varphi_{k'})$ with $m, n = 0 \ldots 6$, and $W_{ss}^{ss}, W_{aa}^{ss}, W_{as}^{sa}$ depend on the difference $\varphi_k - \varphi_{k'}$ while $W_{sa}^{sa}(\varphi_k, \varphi_{k'})$ does not.

The correlator properties Eqs. (5) allowed us to decouple partly Eqs. (3) and derive independent equations for the Cooperons C_+ and C_- as well as two coupled equations for

the Cooperons C_1 and C_2 defined as

$$
\begin{aligned}
C_+ &= C_{aa}^{ss} - C_{sa}^{as} = -\left(C_{as}^{sa} - C_{ss}^{aa}\right), \\
C_- &= C_{aa}^{ss} + C_{sa}^{as} = C_{as}^{sa} + C_{ss}^{aa}, \\
C_1 &= C_{ss}^{ss} = \left(C_{aa}^{aa}\right)^*, \quad C_2 = C_{as}^{as} = \left(C_{sa}^{sa}\right)^*.
\end{aligned}
\tag{6}
$$

The equations are as follows:

$$
\begin{aligned}
C_\pm(\varphi_k,\varphi_{k'},\boldsymbol{q}) &= W_{aa}^{ss}(\theta) \mp W_{as}^{sa}(\theta) + \int_0^{2\pi} \frac{d\varphi_1}{2\pi} P(\varphi_1,\boldsymbol{q}) \\
&\times \left[W_{aa}^{ss}(\theta_1) \mp W_{as}^{sa}(\theta_1)\right] C_\pm(\varphi_1,\varphi_{k'},\boldsymbol{q}),
\end{aligned}
\tag{7}
$$

$$
\begin{aligned}
&C_1(\varphi_k,\varphi_{k'},\boldsymbol{q}) \\
&= W_{ss}^{ss}(\theta) + \int_0^{2\pi} \frac{d\varphi_1}{2\pi} P(\varphi_1,\boldsymbol{q}) \left[W_{ss}^{ss}(\theta_1) C_1(\varphi_1,\varphi_{k'},\boldsymbol{q})\right. \\
&\left. + W_{sa}^{sa}(\varphi_k,\varphi_1) C_2(\varphi_1,\varphi_{k'},\boldsymbol{q})\right],
\end{aligned}
\tag{8}
$$

$$
\begin{aligned}
&C_2(\varphi_k,\varphi_{k'},\boldsymbol{q}) \\
&= W_{as}^{as}(\theta) + \int_0^{2\pi} \frac{d\varphi_1}{2\pi} P(\varphi_1,\boldsymbol{q}) \left[W_{as}^{as}(\varphi_k,\varphi_1) C_1(\varphi_1,\varphi_{k'},\boldsymbol{q})\right. \\
&\left. + W_{aa}^{aa}(\theta_1) C_2(\varphi_1,\varphi_{k'},\boldsymbol{q})\right].
\end{aligned}
\tag{9}
$$

Here we introduced $\theta = \varphi_k - \varphi_{k'}$ and $\theta_1 = \varphi_k - \varphi_1$.

We have found the Cooperons C_+, C_-, C_1, and C_2 expanding them in Fourier series which transfers the integral Eqs. (7)–(9) to systems of linear equations. Since the correlators have a finite number of Fourier harmonics, the linear equation systems are finite: 7 independent equations for both C_+ and C_-, and 14 coupled equations for C_1 and C_2. The Cooperon Fourier harmonics have been found by a numerical solution of these linear equation systems. In the diffusion approximation, q assumed to be small, and $P(\varphi,q)$ is expanded up to q^2 terms.[13–15] This simplifies greatly Eqs. (7)–(9) because only the zeroth and first Fourier harmonics contribute to the Cooperon in the diffusion approximation.

The found Cooperons allowed us to calculate the WL conductivity correction σ. It is well known that this correction is given by a sum of two maximally crossed diagrams. Accordingly, it equals to a sum of two terms $\sigma = \sigma_a + \sigma_b$, where σ_a arises from the backscattering processes and σ_b contribution is due to coherent scattering by arbitrary angles. These corrections are expressed via the Cooperons as follows:

$$
\begin{aligned}
\sigma_a &= -\frac{e^2(v_F\tau_1)^2}{2\pi\hbar} \int \frac{d^2q}{(2\pi)^2} \int_0^{2\pi} \frac{d\varphi}{2\pi} P(\varphi,\boldsymbol{q}) \\
&\times \left\{C_-^{(3)}(\varphi,\varphi+\pi,\boldsymbol{q}) - C_+^{(3)}(\varphi,\varphi+\pi,\boldsymbol{q})\right. \\
&\left. + 2\mathrm{Re}\left[C_1^{(3)}(\varphi,\varphi+\pi,\boldsymbol{q})\right]\right\},
\end{aligned}
\tag{10}
$$

$$
\begin{aligned}
\sigma_b &= -\frac{e^2(v_F\tau_1)^2}{\pi\hbar} \int \frac{d^2q}{(2\pi)^2} \int_0^{2\pi} \frac{d\varphi}{2\pi} P(\varphi,\boldsymbol{q}) \cos\varphi \\
&\times \int_0^{2\pi} \frac{d\varphi'}{2\pi} P(\varphi',\boldsymbol{q}) \cos\varphi' \left\{\sum_\pm \left[W_{aa}^{ss}(\theta) \mp W_{as}^{sa}(\theta)\right]\right. \\
&\times C_\pm^{(2)}(\varphi,\varphi',\boldsymbol{q}) + 2\mathrm{Re}\left[W_{ss}^{ss}(\theta)C_1^{(2)}(\varphi,\varphi',\boldsymbol{q})\right] \\
&\left. + 2\mathrm{Re}\left[W_{sa}^{sa}(\varphi,\varphi')C_2^{(2)}(\varphi,\varphi',\boldsymbol{q})\right]\right\}.
\end{aligned}
\tag{11}
$$

Here $\theta = \varphi - \varphi'$, the upper index (2) and (3) indicates that the diagrams are started from 2 and 3 impurity lines, and the factor τ_1^2 comes from the renormalization of two vertexes due to the scattering anisotropy.

IV. CALCULATION RESULTS AND DISCUSSION

The results of calculation of the WL conductivity correction is shown in Fig. 2. The time $\tau(0)$ is the relaxation time at $k = 0$, cf. Fig. 1. The WL to WAL transition with increase of the hole density is clearly seen for $\tau(0)/\tau_\phi \leqslant 0.04$. It occurs at $k_F a \approx 2$ which corresponds to the density $p \approx 7 \times 10^{11}$ cm^{-2} for the quantum well width $a = 100$ Å. However, Fig. 2 demonstrates that the conductivity is a nonmonotonous function of the hole density which changes sign and become again negative at high $k_F a$ for shorter dephasing times τ_ϕ. Inset in Fig. 2 shows the backscattering and nonbackscattering contributions, σ_a and σ_b.

The backscattering contribution dominates for all values of the parameter $k_F a$. This can be explained by the approximate relation

$$
\sigma_b \approx -\frac{\tau_1 - \tau_0}{\tau_1} \sigma_a,
$$

which is derived in the diffusion approximation.[13,15] The difference between τ_1 and τ_0 is nonzero, but it does not exceed 30%, see Fig. 1. Therefore the nonbackscattering contribution σ_b does not reach the large value $(e^2/2\pi^2\hbar)\ln(\tau_\phi/\tau_1)$. In contrast, it does not exceed the value at $k = 0$ where $\sigma_b = (e^2/2\pi^2\hbar)\ln 2$, see Fig. 2.

In order to explain qualitatively the nonmonotonous behavior of the conductivity correction with the hole density we also compare the results of our exact calculation with ones obtained in the diffusion approximation:

$$
\sigma_a \approx \frac{e^2}{4\pi^2\hbar} \left[2\ln\left(\frac{\tau_1}{\tau_{s\|}} + \frac{\tau_1}{\tau_\phi}\right) + \ln\left(\frac{\tau_1}{\tau_{s\perp}} + \frac{\tau_1}{\tau_\phi}\right) - \ln\frac{\tau_1}{\tau_\phi}\right].
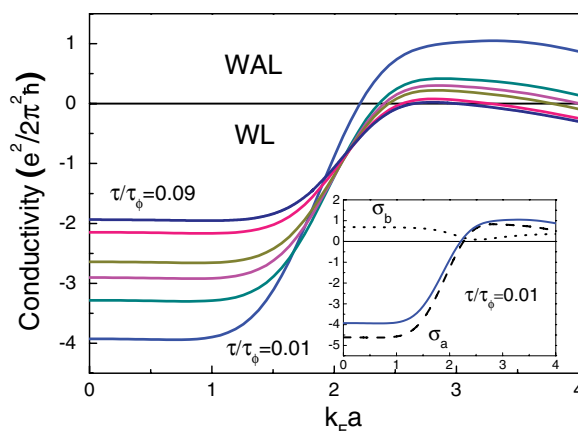\tag{12}
$$

FIG. 2. (Color online) Conductivity correction as a function of hole density at $\tau(0)/\tau_\phi = 0.01, 0.02, 0.04$, and 0.09. Inset: the backscattering (σ_a) and nonbackscattering (σ_b) contributions.
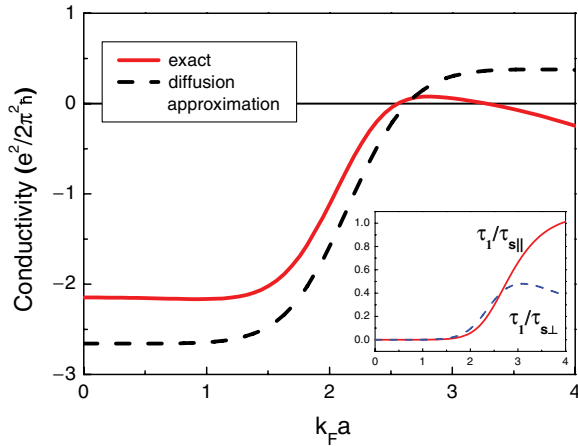
FIG. 3. (Color online) The backscattering correction at $\tau(0)/\tau_\phi = 0.07$ calculated exactly (solid line) and in the diffusion approximation (dashed line). Inset: spin relaxation rates.
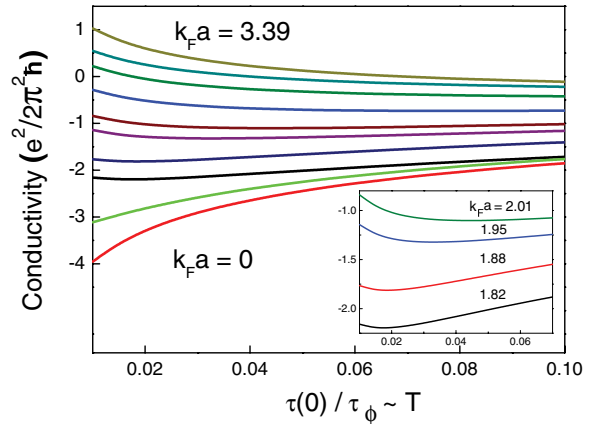

FIG. 4. (Color online) The temperature dependence of the conductivity correction at different hole densities. Inset highlights the region where the conductivity has a minimum.

Here the longitudinal and the transverse spin relaxation rates are given by[8]

$$\frac{1}{\tau_{s\|}} = \frac{1}{\tau_0} - \frac{2\pi}{\hbar} g \int_0^{2\pi} \frac{d\theta}{2\pi} \langle V_{ss}^2(\theta) \rangle,$$

$$\frac{1}{\tau_{s\perp}} = \frac{4\pi}{\hbar} g \int_0^{2\pi} \frac{d\theta}{2\pi} \langle |V_{sa}(\theta)|^2 \rangle.$$

The dependence Eq. (12) is shown in Fig. 3 together with the result of the exact calculation. The increase of the WL correction at $0 < k_F a < 3$ is described by fast increase of both spin relaxation rates which makes smaller the two first logarithmic terms in Eq. (12). This demonstrates that WL to WAL transition in hole systems at long dephasing times is driven by increase of spin-orbit coupling with increase of the hole density. However, at $k_F a > 3$ the WL correction calculated in the diffusion approximation saturates at the value smaller than $(e^2/4\pi^2\hbar)\ln(\tau_\phi/\tau_1)$ obtained in the limit of very fast spin relaxation. This is caused by decrease of the transverse spin relaxation rate $1/\tau_{s\perp}$ and by saturation of the longitudinal rate $1/\tau_{s\|}$, see inset to Fig. 3.

This behavior of the spin relaxation rates at $ka > 1$ can be explained by considering the limit of a very wide quantum well. The coefficients $v_{0\ldots3}$ in Eqs. (1) and (2) in this limit are $v_0 = 1/2$, $v_1 = v_3 = 0$, $v_2 = \sqrt{3}/2$,[20] so the symmetrical and asymmetrical wave functions have the following forms:

$$F_{s,a} = \cos\left(\frac{\pi z}{a}\right)\frac{\exp(\pm i\varphi_k)}{\sqrt{a}}$$
$$\times [(Y\cos\varphi_k - X\sin\varphi_k)s_\pm + iZe^{\pm i\varphi_k}s_\mp].$$

These wave functions correspond to the angular momentum projections $\pm 3/2$ on the direction of $\mathbf{k}$ in the structure plane as it should be at large ka. Calculating the scattering matrix elements $V_{ss} = V_0\langle F_{s\mathbf{k}'}|F_{s\mathbf{k}}\rangle$ and $V_{sa} = V_0\langle F_{s\mathbf{k}'}|F_{a\mathbf{k}}\rangle$ we derive that at $ka \to \infty$

$$1/\tau_{s\perp} = 0, \quad 0.9\tau_{s\|} = \tau_0 = \tau_1.$$

Infinite $\tau_{s\perp}$ shows that the hole spin relaxation is suppressed not only at small but also at large ka. According to the

calculation results shown in the inset to Fig. 3 this limiting case is almost realized at $k_F a \leqslant 4$ when only the ground subband is occupied. Therefore the first logarithmic term in Eq. (12) is small at $k_F a \sim 4$ while the second one increases partially compensating the last term, and the total correction saturates. Moreover, in contrast to the diffusion-approximation result, the exactly calculated WL correction totally repeats the behavior of $\tau_1/\tau_{s\perp}$: The above derived suppression of hole spin relaxation in wide quantum wells is reproduced in the WL conductivity correction as it is seen from the exact calculation result shown in Fig. 3 which has a maximum and decreases at larger ka.

We have also calculated the WL conductivity correction as a function of temperature $T \sim \tau_\phi^{-1}$ at different hole densities. The result shown in Fig. 4 demonstrates the transition from metal to insulator temperature behavior. This transition is due to spin-orbit interaction which is present even in symmetrical quantum wells with the degenerate hole energy spectrum. The inset to Fig. 4 shows nonmonotonous temperature dependence at moderate hole densities.

V. SUMMARY

To summarize, we have developed WL theory for holes in quantum wells taking into account both ballistic and diffusion processes. The conductivity correction is calculated in a wide range of hole densities and temperatures taking into account real nonparabolicity of the energy spectrum. WL instead of WAL can occur at high densities due to suppression of hole spin relaxation at large in-plane wavevectors. The transition from metal to insulating temperature behavior is demonstrated in the symmetrical quantum well with spin-degenerate hole subbands. Such a transition can be detected by magnetoconductivity measurements. This mechanism can concur with the mechanism due to Rashba splitting of hole energy spectrum which has been used in Ref. 11 for explanation of WL experiments on two-dimensional hole systems. Dresselhaus spin-orbit interaction can also lead to WAL. Theoretically the Dresselhaus coupling for two-dimensional holes can be taken into account by k^3 spin-orbit splitting. This problem has

been solved in Ref. 23 where it was demonstrated that WAL takes place if the Dresselhaus splitting is larger than the elastic scattering rate $\hbar/\tau$. The calculations performed in Ref. 21 for a diffusive strip show only positive magnetoconductivity at $ka = 2$ which agrees with our results. Our Figs. 2 and 4 predict transition to WAL at higher $ka \sim 3$ for long dephasing times.

*golub@coherent.ioffe.ru

[1] S. Das Sarma, S. Adam, E. H. Hwang, and E. Rossi, Rev. Mod. Phys. **83**, 407 (2011).

[2] E. B. Olshanetsky, Z. D. Kvon, G. M. Gusev, N. N. Mikhailov, S. A. Dvoretsky, and J. C. Portal, JETP Lett. **91**, 347 (2010) [Pis'ma Zh. Exp. Teor. Fiz. **91**, 375 (2010)].

[3] J. Chen, X. Y. He, K. H. Wu, Z. Q. Ji, L. Lu, J. R. Shi, J. H. Smet, and Y. Q. Li, Phys. Rev. B **83**, 241304 (2011).

[4] H.-T. He, G. Wang, T. Zhang, I.-K. Sou, G. K. L. Wong, J.-N. Wang, H.-Zh. Lu, S.-Q. Shen, F.-Ch. Zhang, Phys. Rev. Lett. **106**, 166805 (2011).

[5] G. M. Minkov, A. V. Germanenko, O. E. Rut, A. A. Sherstobitov, S. A. Dvoretski, and N. N. Mikhailov, Phys. Rev. B **85**, 235312 (2012).

[6] G. Tkachov and E. M. Hankiewicz, Phys. Rev. B **84**, 035444 (2011).

[7] M. O. Nestoklon, N. S. Averkiev, and S. A. Tarasenko, Solid State Commun. **151**, 1550 (2011).

[8] L. E. Golub and S. Pedersen, Phys. Rev. B **65**, 245311 (2002).

[9] M. Y. Simmons, A. R. Hamilton, M. Pepper, E. H. Linfield, P. D. Rose, and D. A. Ritchie, Phys. Rev. Lett. **84**, 2489 (2000).

[10] Y. Y. Proskuryakov, A. K. Savchenko, S. S. Safonov, L. Li, M. Pepper, M. Y. Simmons, D. A. Ritchie, E. H. Linfield, and Z. D. Kvon, J. Phys. A: Math. Gen. **36**, 9249 (2003).

[11] G. M. Minkov, A. A. Sherstobitov, A. V. Germanenko, O. E. Rut, V. A. Larionova, and B. N. Zvonkov, Phys. Rev. B **71**, 165312 (2005).

[12] G. M. Minkov, A. V. Germanenko, O. E. Rut, A. A. Sherstobitov, and B. N. Zvonkov, Phys. Rev. B **75**, 193311 (2007).

[13] N. S. Averkiev, L. E. Golub, and G. E. Pikus, Zh. Exp. Teor. Fiz. **113**, 1429 (1998) [JETP **86**, 780 (1998)].

[14] N. S. Averkiev, L. E. Golub, and G. E. Pikus, Solid State Commun. **107**, 757 (1998).

[15] N. S. Averkiev, L. E. Golub, and G. E. Pikus, Fiz. Techn. Poluprov. **32**, 1219 (1998) [Semiconductors **32**, 1087 (1998)].

[16] S. Pedersen, C. B. Sørensen, A. Kristensen, P. E. Lindelof, L. E. Golub, and N. S. Averkiev, Phys. Rev. B **60**, 4880 (1999).

[17] V. M. Gasparyan and A. Yu. Zyuzin, Fiz. Tverd. Tela (Leningrad) **27**, 1662 (1985) [Sov. Phys. Solid State **27**, 999 (1985)].

[18] A. P. Dmitriev, V. Yu. Kachorovskii, and I. V. Gornyi, Phys. Rev. B **56**, 9910 (1997).

[19] E. L. Ivchenko and G. E. Pikus, in *Superlattices and Other Heterostructures. Symmetry and Optical Phenomena* (Springer, Berlin, 1997).

[20] I. A. Merkulov, V. I. Perel', and M. E. Portnoi, Zh. Eksp. Teor. Fiz. **99**, 1202 (1991) [Sov. Phys. JETP **72**, 669 (1991)].

[21] V. Krueckl, M. Wimmer, I. Adagideli, J. Kuipers, and K. Richter, Phys. Rev. Lett. **106**, 146801 (2011).

[22] K. S. Romanov and N. S. Averkiev, Zh. Exp. Teor. Fiz. **128**, 811 (2005) [JETP **101**, 699 (2005)].

[23] M. M. Glazov and L. E. Golub, Semicond. Sci. Technol. **24**, 064007 (2009).